This is the accepted manuscript version of the paper: T. Fapanni, E. Sardini, M. Borghetti, M. Serpelloni and S. Bellotti, "Preliminary Results on Fully-Printed and Silver-Based Temperature Sensors for Aerospace Industry," *2023 IEEE International Workshop on Metrology for Industry 4.0 & IoT (MetroInd4.0&IoT)*, Brescia, Italy, 2023, pp. 200-204, doi: 10.1109/MetroInd4.0IoT57462.2023.10180153.The final published version and copyright permissions are available on https://ieeexplore.ieee.org/document/10180153

Preliminary Results on Fully-Printed and Silver-Based Temperature Sensors for Aerospace Industry

Tiziano Fapanni
Department of Information Engineering
University of Brescia
Brescia, Italy
tiziano.fapanni@unibs.it

Michela Borghetti
Department of Information Engineering
University of Brescia
Brescia, Italy
michela.borghetti@unibs.it

Stefano Bellotti
Department of Information Engineering
University of Brescia
Brescia, Italy
s.bellotti004@studenti.unibs.it

Emilio Sardini
Department of Information Engineering
University of Brescia
Brescia, Italy
emilio.sardini@unibs.it

Mauro Serpelloni
Department of Information Engineering
University of Brescia
Brescia, Italy
mauro.serpelloni@unibs.it

***Abstract*— CubeSats are small satellites produced usually by off-the-shelf components that are designed to propose space exploration and research to universities reducing expenses and development time. Since most of their components are commercial and temperatures in space range between -100 °C and 120 °C, the thermal profile of the devices must be considered in the design process to optimize the efficiency and to avoid system failures. Among the different kinds of temperature sensors reported in the literature, the use of printed resistance temperature detectors (RTDs) is interesting to embed the sensor in the structure thus reducing the weight of the satellite. In this frame, the use of innovative Industry 4.0 technologies allows both the improvement of the metrological characteristics of the sensors and the reduction of the costs increasing the material use efficiency. In this work, two aluminum alloys and three plastic were tested as substrates for the development of printed silver-based temperature sensors. The sensors were characterized in the [-10; 100] °C temperature range using both an oven and a climatic chamber in order to assess the resistance at 0 °C, the temperature coefficient of resistance (TCR) as well as the hysteresis of the devices. The results showed that the metallic substrates performed better, with TCRs bigger than 2.5 10^{-3} $°C^{-1}$ and low hysteresis. Among the plastic substrates, Kapton produced the most stable TCRs values with values around 2.3·10-3 $°C^{-1}$. Even though ABS performed similarly (TCR around 2.0·10-3 $°C^{-1}$), it presented linearity and hysteresis issues at high temperatures.**

Keywords— temperature sensors, printed electronics, printed RTD, aerospace sensing

I. Introduction

Space is the new frontier for exploration that is attracting great interest from both researchers and industry. In 1999 a cheap, miniaturized and modular satellite project was proposed by California Polytechnic State University (Cal Poly) and Stanford University in order to promote space research in the universities. Those devices, called CubeSats, are described in the standard "CubeSat design specification" [1] that defines the base unit as a cube of 10 cm with a maximum weight of 1.33 kg. Usually, off-the-shelf electronic components are employed in those nanosatellites to reduce the overall cost and reduce the development and fabrication time. In this frame, the thermal profile of the devices must be taken into account in the design process to optimize the efficiency of the components and to avoid system failures. [2] In the specific application, the temperature variations are mostly related to solar radiation and the power dissipation of components. Solar radiation is the main factor that influences the device's internal temperature, which can thus range between -10 °C and 80 °C. [3]–[6] In order to monitor the device temperatures, sensors are required. Among the possible, different kinds of temperature sensors are reported in the literature. Bryan et al. [7], for instance, present a thermocouple-based system that is able to measure variations in the thermal flux, Gamba et al. [8] employ a surface acoustic wave sensor for temperature detection, while Courts presents both a diode-based device and negative [9] coefficient thermistors (NTC) [11] able to work from room temperature to 20 K or below. However, due to their repeatability, accuracy, quick response times, as well as their wide temperature range, resistive temperature detectors (RTDs), are often chosen in aerospace applications. Moreover, one of the advantages of RTDs over other typologies of temperature sensors is the ease of fabrication by additive manufacturing and, among these techniques, the most promising are the printed ones [10] that allow embedding the sensor directly on the object whose temperature has to be monitored. In fact, using the innovative processes proposed by the Industry 4.0 paradigm, and in particular the additive manufacturing techniques it is possible to obtain a quick prototyping process that can be used to embed sensors on non-planar surfaces. Among the possible additive manufacturing techniques used in printed electronics, aerosol jet printing (AJP) was selected for this study thanks to its fully digital and maskless fabrication process and its flexibility in terms of available viscosity of inks and possible substrates. In this work, a set of materials typically used in aerospace and suitable used as substrate for RTDs were evaluated in order to compare their performances in terms of metrological characteristics and weight.

This work was founded by the FORCE project – "Formation flight of CubEsat Assemblies for Earth observation" (PON ARS01_00922).

II. Related Works

As hinted in the previous section, temperature sensing is crucial in aerospace applications and CubeSats, since accurate measurements are necessary for a wide range of critical operations as well as insure the system well behavior. Among the possible temperature sensors for aerospace applications Courts proposes [11] a cryogenic temperature sensor that can be used from room temperature to 20 K or below. The paper shows how the proposed device has a negative coefficient of temperature and different possible test protocols are proposed. In a different article [12], Zhao et al. propose a novel optical fiber temperature sensor (OFTS) that thanks to its high sensitivity and compact structure is well suited for aerospace applications. Moreover, printed temperature sensors have recently emerged as a promising technology for aerospace applications due to their low-cost, lightweight, and flexible nature. In [13], Liew et al., compare the performance of a low-cost and flexible temperature sensor produced with a custom ink to a sensor printed with a commercial one showing comparable results in a temperature range between 30°C and 100°C. Another example of printed sensor for aerospace is proposed by Gee et al. in [14], where it is proposed a device that could be used as a passive wireless structural health monitoring embedding both a strain and a temperature sensor within a chipless RFID device.

III. Materials and Methods

A. Materials and Design

Different materials employed in the fabrication of CubeSats range from metals and plastics [15]. The former class is widespread in aerospace applications, especially aluminum alloys are the most used materials since they present a good stiffness/weight ratio, easy machining, low density and cost [15]. On the other hand, plastic materials seem promising as novel materials in aerospace because they are insulators and thanks to their low density and their thermos-chemical characteristics, as well as their rapid prototyping [16], [17]. All those materials are thus suitable substrates to embed printed sensors in aerospace applications. Thus, in this work, two aluminum alloys (AlSi7Mg and HE30TF) and three plastic materials - polyether ether ketone (PEEK), acrilonitrile butadiene styrene (ABS) and Kapton - were selected as possible substrates for printed silver-based temperature sensors. The devices were fabricated using the ink Metalon HPS-108AE1 (Novacentrix, Austin, Texas, USA) deposited through AJP, which uses a three-gas flows fluid dynamic system to atomize the ink (atomizer flow), control the dimension of the particles (exhaust flow) and focus the aerosol on the nozzle (sheath flow) [18].

The sensors were designed to be a serpentine of 174.5 mm with two rectangular pads of 2 mm x 1 mm to easily connect the devices to the measurement instrumentation (Fig. 1). The target linewidth selected is 300 µm to achieve resistances around 50 Ω.

B. Fabrication Process

As regards the fabrication process, the first step was the substrate preparation. The substrates were carefully cleaned to remove any grease on the surface and thus improving the ink-substrate adhesion. Moreover, to isolate the conductive ink layer from the metallic substrates, the metallic substrates were coated with a bi-component epoxy resin (193.R7042, Vernici Caldart S.R.L., Bellusco, Italy) and oven cured at 80 °C for 30 minutes. Then, the conductive silver ink was deposited on the prepared substrate by AJP and cured. The sintering process was performed in an oven at 180°C for one hour for all the samples, except the ones fabricated on ABS, which were cured through a PulseForge 1300 system (Novacentrix, Austin, Texas, USA) to preserve the integrity of ABS during the thermal sintering of the silver ink. The sensors were then wired in a four wires configuration using a conductive epoxy CW2400 (Chemtrionics, Kennsaw, Georgia, USA). In order to shield the printed tracks from the environmental agents, two different coatings were tested: a lacquer (RS Pro Printed CCT Board Lacquer RS 136-8533) and a silicon-based resin (RS Modified Silicone Conformal Coating Aerosol RS 494-714). Both were sprayed on top of the samples. Each coating was used on 3 samples for each substrate. A few examples of the fully produced samples are shown in Fig. 1.

Fig. 1. Example of the produced samples on HE30TF substrate coated with the two coatings: resin (left) and lacquer (right)

C. Process Evaluation

The fabrication process was evaluated by verifying the electrical conductivity between the two pads with a Hewlett–Packard 34401A (HP, Palo Alto, CA, USA) digital multimeter and by measuring the profile in three different positions of the printed tracks through an Alpha-Step IQ Surface Profilometer (KLA-Tencor, Milpitas, CA, USA). The achieved data were processed using MATLAB in order to estimate the average width, thickness and area of the printed tracks. That information was then used to estimate the resistivity of the printed ink that was compared to the one provided by the ink manufacturer.

D. Evaluation in Temperature

The evaluation in temperature was performed using both a ThermoScientific VACUTherm Oven (Thermo Electron LED GmbH, Langenselbold, Germany) and a climatic chamber UC 150/70 (Advanced Material Testing S.R.L., Limbiate, Italy) to be able to cover the overall range of [-10; 100] °C. The oven was set to cover the [+30; 100] °C range in 10 °C steps that lasted 30 minutes each, while the climatic chamber covered the range [-10; 40] °C with 5 °C steps that lasted 30 minutes each. In both configurations, the sensors

under test were placed in a box to limit the effects of internal ventilation and changes in humidity. The internal temperature of the box was sampled using a commercial Pt100 with nominal accuracy of ±0.1 °C at 0 °C. The response of the sensors was considered linear and the collected data were processed in order to use a first-order model for defining the relationship between the resistance and the temperature, as in (1)

$$R(T)=R_0(1+\alpha T) \qquad (1)$$

where the resistance of the sensor (R) at T temperature is related to the resistance measured at 0 °C (R_0), while the temperature coefficient of resistance (TCR) is indicated as α.

IV. Results and Discussion

A. Process Evaluation

At first, the electrical conductivity of the printed was tested to verify the fabrication process. The achieved measurements showed a mean value of 48.5 **Ω**, perfectly in accordance with the design, the ink specifications, while the coefficient of variation is in accordance with the fabrication process variability. Then, to further evaluate the fabrictaion process, the profile of the printed tracks on Kapton was evaluated and the resistivity of the material was found. The mean profile obtained as mean value of the measures performed in three positions for all the lines (24 tracks in total) is shown in Fig. 2. In that, it is possible to observe a coffee-ring effect in the form of a non-perfectly even top layer. The measurements revealed an average thickness of (2.19 ± 0.32) µm. To estimate the active surface of the printed track, the track was assumed a trapezoid and the mean trace width at 10% and 90% of the maximum height were calculated. The biggest base is 398 µm and the smallest one is 183 µm for a total surface area of 636 μm^2. With this information, the resistivity of the deposited ink results $20 \cdot 10^{-6}$ **Ω**·cm, which is a value in accordance with the specifications provided by the manufacturer.

B. Evaluation in Temperature

The evaluation in temperature allowed us to compare the behavior of the different produced sensors. The raw data were processed to extract the calibration lines shown in Fig. 3 where it's possible to notice a fair linear relationship between the obtained resistance and the imposed temperature. Moreover, from the collected data the temperature coefficient of resistance (TCR) and the resistance at 0 °C (R_0) were estimated and reported in Table I. In general, the metallic substrates contribute to a higher mean TCR and lower R_0 values. Moreover, it was observed a substantial difference in the TCR of samples coated with the resin and the lacquer. In fact, the resin improved the TCR up to 20% and lowered the

TABLE I: Obtained average TCR and R_0 values for each material

	TCR ($\cdot 10^{-4}$ °C^{-1})	**R_0 (Ω)**
HE30TF	25.7±3.7	31.8±9.3
AlSi7Mg	28.8±3.8	35.9±9.6
PEEK	21.0±1.9	67.1±15.2
ABS	20.3±3.0	104.0±93.7
Kapton	23.4±1.0	43.0±16.9

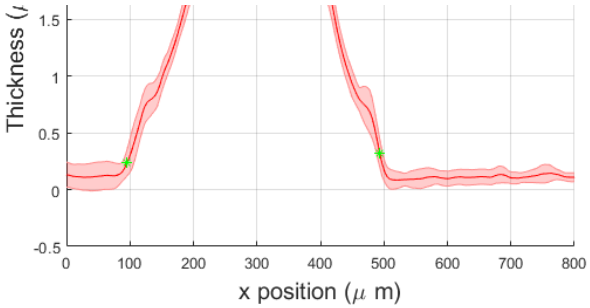

Fig. 2. Profile of the printed track on Kapton obtained with the mechanical profilometer. Solid red line depicts the mean value, shaded red represents the standard deviation calculated on X samples while green asterisks/circles depicts the points t\hat identificates the 90% and the 10% of the curve used to obtain the top and bottom width of the printed track.

R_0 up to -65% with respect to the lacquer for the samples produced on HE30TF, AlSi7Mg and PEEK. The effect observed on ABS, however, is in contrast with the one of the other materials. In fact, it presents an increase of R_0 around 24% and the TCR decreases of 10% changing the lacquer for the resin. This different behavior as well as the higher average achieved resistance in the ABS samples is probably related to the different sintering process that has to be improved to better the functionality of the devices.

The hysteresis of the devices was evaluated considering both rising and falling temperatures in both experimental setups. An example of the behavior of a sensor printed on ABS is shown in Fig. 4. The collected data were processed to analyze the changes in the fitting parameters (TCR and R_0). R_0 presents variations below 2% in most substrate-coating pairs, except for the ones on ABS. TCR variations are wider and mostly different between the different substrates. In particular, metallic substrates behave similarly, but with differences of 4% in TCR in the falling/rising. On the other hand, the plastic substrates present widely different behaviors. Kapton shows small differences in all the testing conditions. Otherwise, PEEK shows changes between 5% and 12% in

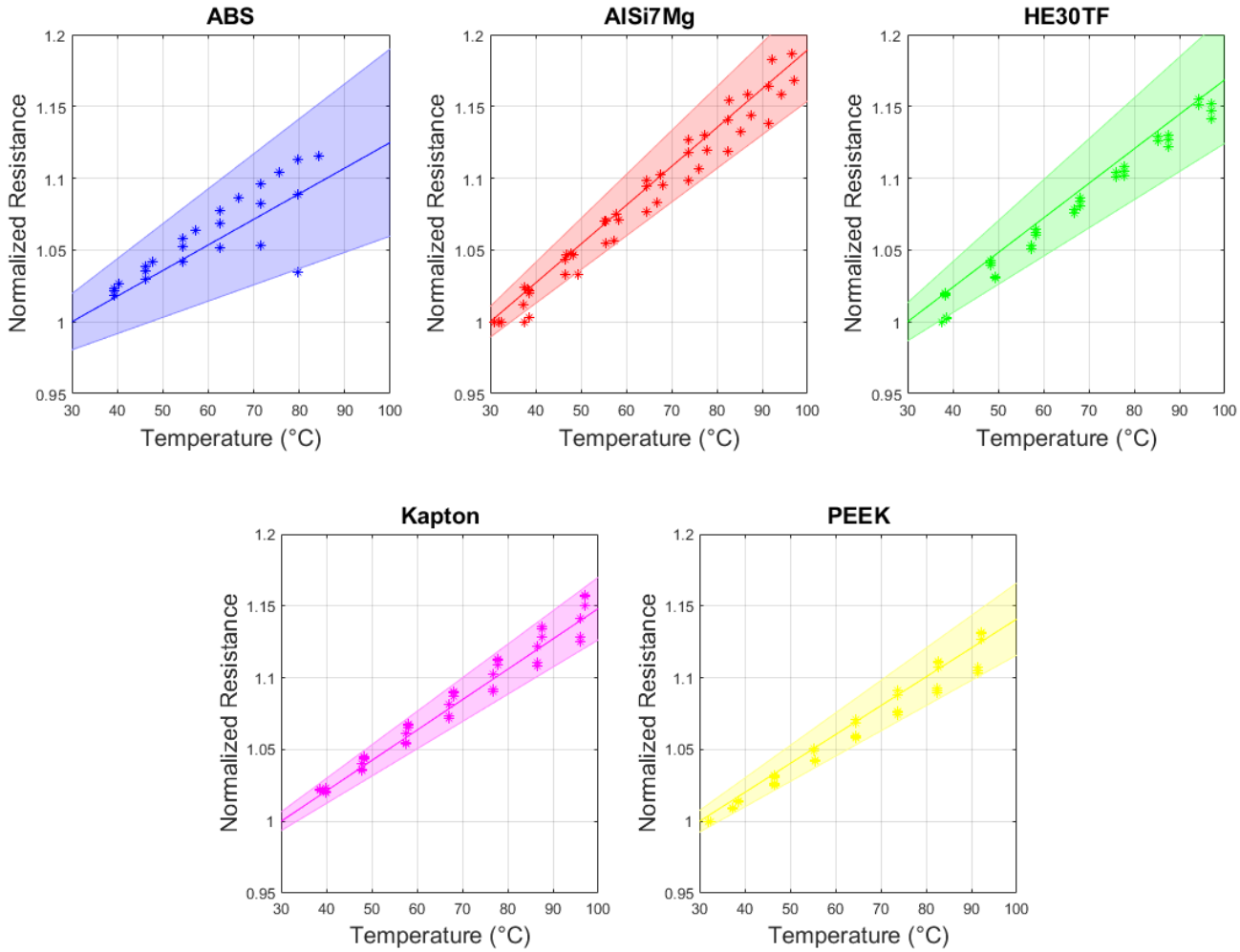

Fig. 3. Change in resistance related to temperature obtained from the data achieved with the oven. Asterisks depicts the experimental data, solid lines the average calibration line and the shaded area depict the standard deviation of the obtained mean.

TCR, considering the different coatings (lacquer and resin respectively). Lastly, ABS presents a peculiar behavior. In fact, at low temperature it presents almost negligible differences in falling/rising TCR, but when exposed at higher temperatures it presents changes up to 21%. The hereby described effects can also be summarized by a hysteresis parameter that was estimated considering the largest difference between the best fitting line and the experimental data in the temperature range ([-10 ; 40] °C for the climatic chamber, [30 ; 100] °C for the oven). In general, the experiment carried out in the oven produced smaller hysteresis than the ones executed in the climatic chamber. That might be due to the forced cooling provided by the climatic chamber that reduces the homogeneity of temperature in the chamber producing discrepancies between the temperature measured by feedback Pt100 and the sensors under test. However, as said before, the effects on ABS of higher temperatures are evident and produce increases of the hysteresis parameters up to 3.65 times. All the achieved hysteresis coefficients are shown in Table II.

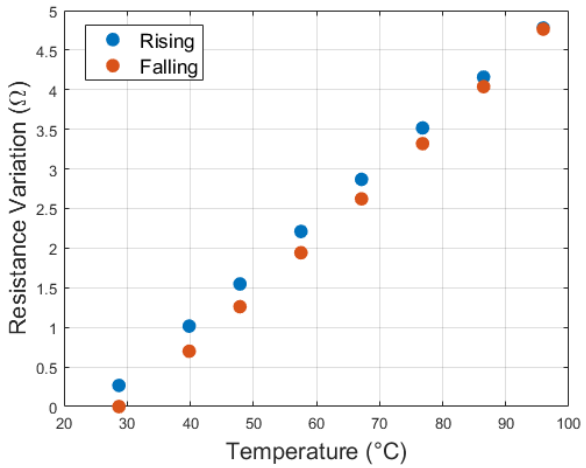

Fig. 4. Example of the measured difference in the behavior of the sensors while applying rising (blue) or decreasing (red) temperature gradients. In particular the presented data were collected on a ABS sensor.

C. *Sintering Influence*

In the previously described evaluations, two sensors resulted defective presenting strongly non-linear behaviors and were

TABLE III: Re-sintering effects shown in terms of sensitivity, resistance at 0°C and linearity (R^2)

	TCR (°C $^{-1}$)	R_0 (Ω)	R^2
Test 1	0.0011	89.9	0.9663
Test 2	0.0019	82.3	0.9997
Test 3	0.0020	81.1	0.9999

thus excluded from the analysis. The observed effects were due to a non-perfect sintering process that led to re-sintering during the characterization. To better assess this effect, one of the samples (PEEK substrate, coated in lacquer) was exposed to the characterization process in the oven three times. Looking at the results in time (Fig. 5a), the behavior for the low temperature steps is similar between the three tests that present three different offsets. However, looking at the last steps, it is possible to observe a wide difference between test 1, which does not reach a stable level but presents a decreasing slope, and the others that reaches a stable level. Moreover, considering the temperature-resistance calibration line (Fig. 5b) different aspects could be observed. Again, the average room temperature resistance of the device decreases after each test. The collected data were fitted using again the model described in (1) and the resulting fitting values are reported in Table III. From those, it's evident how the re-sintering positively impacts both the TCR that after the third test reaches values comparable to the average ones of the other samples and the linearity of the calibration line with a hysteresis coefficient that is lowered 8 times.

V. Conclusions

In this work the suitability of different metallic and plastic materials as substrates for printed temperature sensors in aerospace applications was evaluated. The RTD sensors were produced with a nanoparticle-based silver ink by Novacentrix using aerosol jet printing, which allows both great spatial resolution and a quick product development even on 3D substrates. The printed tracks presented an average linewidth of 398 µm and thickness of 2.19 µm that produced a room temperature resistance of 48.5 Ω on average. The sensors were then divided into two groups each of which was coated to avoid degradation with one of two different materials: a lacquer or a resin. Then, the sensors were evaluated in temperature in the range [-10; 100] °C using a combination of an oven and a climatic chamber in order to assess the resistance at 0 °C, the temperature coefficient of resistance (TCR) as well as the hysteresis of the devices. In general, the metallic substrates performed better, with TCRs bigger than $2.5 \cdot 10^{-3}$ $°C^{-1}$ and the lowest hysteresis. Among the plastic substrates, Kapton produced the most stable TCRs values with values around $2.3 \cdot 10^{-3}$ $°C^{-1}$. Even though, ABS performed similarly (TCR≈$2.0 \cdot 10^{-3}$ $°C^{-1}$) presented issues at high temperatures compromising the linearity and increase the hysteresis of the sensors.

Acknowledgments

The authors wish to thank Danilo Febbrari and Alberto Tiburzi for their support in the development of the research.

References

[1] California Polytechnic State University, *Cubesat Design Specification Rev 14.1*, vol. 8651, no. February. 2022.

[2] J. R. Wertz and W. J. Larson, "Space Mission Analysis and Design (third edition)," p. 1010, 1999.

[3] D. V. Schatzel, "Improving heat transfer performance of printed circuit boards," *IEEE Aerosp. Conf. Proc.*, pp. 1–6, 2009, doi: 10.1109/AERO.2009.4839529.

[4] R. Stevenson Soler Chisabas, G. Loureiro, C. de Oliveira Lino, and D. F. Cantor, "Method for CubeSat Thermal-Vacuum Cycling Test Specification," *47th Int. Conf. Environ. Syst.*, no. July, pp. 1–15, 2017.

[5] J. Friedel and S. McKibbon, "Thermal Analysis of the CubeSat CP3 Satellite," *Aerosp. Eng.*, no. March, p. 22, 2011, [Online]. Available: http://digitalcommons.calpoly.edu/aerosp/46/.

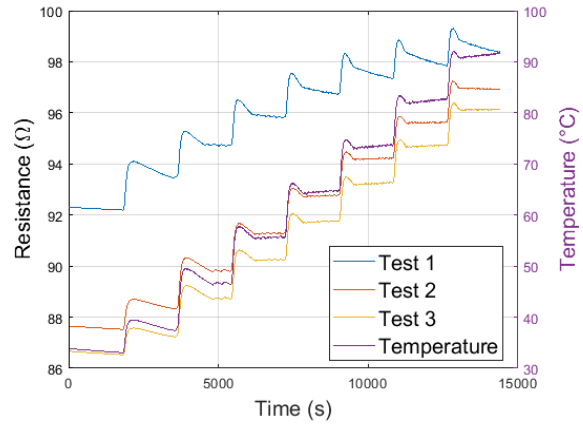

(a)

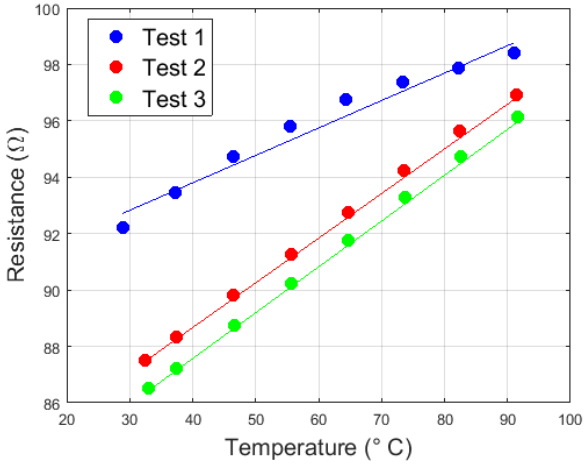

(b)

Fig. 5. Effects of different sintering conditions that could affect the devices in time domain (a) and reported in a calibration line (b) where circles represent the experimental data and the lines are the best fitting of equation 1.

[6] K. Thanarasi, "Thermal Analysis of CUBESAT in Worse Case Hot and Cold Environment Using FEA Method," *Appl. Mech. Mater.*, vol. 225, pp. 497–502, Nov. 2012, doi: 10.4028/www.scientific.net/AMM.225.497.

[7] B. S. Elkins, M. Huang, and J. I. Frankel, "Higher-time derivative of in-depth temperature sensors for aerospace heat transfer," *Int. J. Therm. Sci.*, vol. 52, no. 1, pp. 31–39, 2012, doi: 10.1016/j.ijthermalsci.2011.09.018.

[8] P. Gamba *et al.*, "Wireless passive sensors for remote sensing of temperature on aerospace platforms," *IEEE Sens. J.*, vol. 14, no. 11, pp. 3883–3892, 2014, doi: 10.1109/JSEN.2014.2353623.

[9] S. S. Courts, "A new cryogenic diode thermometer," pp. 1620–1627, 2003, doi: 10.1063/1.1472198.

[10] T. Fapanni, E. Sardini, and M. Serpelloni, "A Preliminary Study on Flexible Temperature Sensors for Eskin Medical Devices," 2022.

[11] S. S. Courts, "A standardized Cernox™ cryogenic temperature sensor for aerospace applications," *Cryogenics (Guildf).*, vol. 64, pp. 248–254, 2014, doi: 10.1016/j.cryogenics.2014.03.009.

[12] X. Zhao *et al.*, "Sensitivity-enhanced temperature sensor utilizing core offset and hollow core Bragg fiber," *Opt. Fiber Technol.*, vol. 75, no. August 2022, p. 103165, 2023, doi: 10.1016/j.yofte.2022.103165.

[13] Q. J. Liew, A. S. A. Aziz, H. W. Lee, M. W. Lee, H. F. Hawari, and M. H. Md Khir, "Inkjet-Printed Flexible Temperature Sensor

Based on Silver Nanoparticles Ink †," *Eng. Proc.*, vol. 2, no. 1, pp. 2–7, 2020, doi: 10.3390/ecsa-7-08216.

[14] K. Mc Gee, P. Anandarajah, and D. Collins, "Use of Chipless RFID as a Passive, Printable Sensor Technology for Aerospace Strain and Temperature Monitoring," *Sensors*, vol. 22, no. 22, 2022, doi: 10.3390/s22228681.

[15] E. A. Slejko, A. Gregorio, and V. Lughi, "Material selection for a CubeSat structural bus complying with debris mitigation," *Adv. Sp. Res.*, vol. 67, no. 5, pp. 1468–1476, 2021, doi: 10.1016/j.asr.2020.11.037.

[16] J. Piattoni, G. P. Candini, G. Pezzi, F. Santoni, and F. Piergentili, "Plastic Cubesat: An innovative and low-cost way to perform applied space research and hands-on education," *Acta Astronaut.*, vol. 81, no. 2, pp. 419–429, 2012, doi: 10.1016/j.actaastro.2012.07.030.

[17] A. Takacs, S. Charlot, P. Calmon, and D. Dragomirescu, "VHF/UHF Kapton supported antenna for cubesat applications," *2017 IEEE Antennas Propag. Soc. Int. Symp. Proc.*, vol. 2017-Janua, pp. 2485–2486, 2017, doi: 10.1109/APUSNCURSINRSM.2017.8073285.

[18] M. Borghetti, E. Cantù, E. Sardini, and M. Serpelloni, "Future sensors for smart objects by printing technologies in Industry 4.0 scenario," *Energies*, vol. 13, no. 22, 2020, doi: 10.3390/en13225916.